

# A Non-invasive Methodology for Fetal Monitoring during Pregnancy

E. C. Karvounis<sup>1</sup>; M. G. Tsipouras<sup>1</sup>; C. Papaloukas<sup>2</sup>; D. G. Tsalikakis<sup>1</sup>; K. K. Naka<sup>4, 5</sup>; D. I. Fotiadis<sup>1, 3, 4</sup>

<sup>1</sup>Unit of Medical Technology and Intelligent Information Systems, Department of Materials Science and Engineering, University of Ioannina, Ioannina, Greece;

<sup>2</sup>Department of Biological Applications and Technology, University of Ioannina, Ioannina, Greece;

<sup>3</sup>Biomedical Research Institute – FORTH, Ioannina, Greece;

<sup>4</sup>Michaelidion Cardiology Center, Ioannina, Greece;

<sup>5</sup>Department of Cardiology, Medical School, University of Ioannina, Ioannina, Greece

## Keywords

Fetal ECG, heart rate, blind source separation, fetal monitoring, ST analysis

## Summary

**Objectives:** This paper describes a methodology for the monitoring of the fetal cardiac health status during pregnancy, through the effective and non-invasive monitoring of the abdominal ECG signals (abdECG) of the mother.

**Methods:** For this purpose, a three-stage methodology has been developed. In the first stage, the fetal heart rate (fHR) is extracted from the abdECG signals, using nonlinear analysis. Also, the eliminated ECG (eECG) is calculated, which is the abdECG after the maternal QRSs elimination. In the second stage, a

blind source separation technique is applied to the eECG signals and the fetal ECG (fECG) is obtained. Finally, monitoring of the fetus is implemented using features extracted from the fHR and fECG, such as the T/QRS ratio and the characterization of the fetal ST waveforms.

**Results:** The methodology is evaluated using a dataset of simulated multichannel abdECG signals: 94.79% accuracy for fHR extraction, 92.49% accuracy in T/QRS ratio calculation and 79.87% in ST waveform classification.

**Conclusions:** The novel non-invasive proposed methodology is advantageous since it offers automated identification of fHR and fECG and automated ST waveform analysis, exhibiting a high diagnostic accuracy.

though fHR monitoring using CTG is still considered the standard of care for intrapartum fetal surveillance [3], CTG data interpretation has remained a subject of scientific controversy; data are interpreted by physicians based on visual recognition of fHR patterns (e.g. bradycardia, accelerations, decelerations) with a high intra- and inter-observer variability, limiting thus the clinical usefulness of the technique. Moreover, although the sensitivity of the method to detect fetal hypoxia is high, its specificity is poor resulting in increased rates of unnecessary medical interventions without noticeable improvement in fetal outcomes [4]. Electronic fHR monitoring by CTG reduces neonatal seizures by 50%, but not fetal mortality, at a price of increased risk of caesarean section and vaginal operative delivery [4].

A lot of scientific work has focused to the development of new methods for continuous intrapartum monitoring aiming to improve both fetal and maternal outcomes. ST waveform analysis of the fetal electrocardiogram (fECG) has been developed to provide objective information about the fetal condition in adjunction to fHR monitoring [5]. Repolarization of myocardial cells is very sensitive to metabolic dysfunction induced by fetal hypoxia. This might be reflected in ST waveform changes in fECG such as an increase in T wave, quantified by the ratio of the T wave to the QRS amplitude (T/QRS ratio), or a biphasic ST pattern. Combining these features with fHR pattern analysis and additional clinical information aids to reduce uncertainty of presence or absence of hypoxia, leading thus to a reduction in unnecessary interventions. Several clinical studies showed a reduction in fetal morbidity when clinical intervention was led by intrapartum fHR monitoring in conjunction with ST waveform analysis

## Correspondence to:

D. I. Fotiadis  
Unit of Medical Technology and Intelligent Information Systems  
Dept. of Materials Science and Engineering  
University of Ioannina  
PO Box 1186  
451 10 Ioannina  
Greece  
E-mail: fotiadis@cs.uoi.gr

Methods Inf Med 2009; 48: ■—■

doi: 10.3414/ME09-01-0041

received: May 12, 2009

accepted: August 26, 2009

republished: November 20, 2009

## 1. Introduction

During pregnancy, the supply of oxygen and nutrients to the fetus and the removal of carbon dioxide and other waste gases is achieved through the placenta. Any alteration in placental function can result in reduced oxygen delivery to the fetus, a condition known as fetal hypoxia, associated with severe perinatal morbidity (metabolic acidosis, encephalopathy) and mortality [1]. Monitoring of the fetus

during pregnancy may enable recognition of pathological conditions such as fetal hypoxia, allowing thus prompt medical interventions before irreversible changes take place.

Fetal heart rate (fHR) monitoring remains the main type of fetal health assessment [2]. Cardiotocography (CTG) is a method widely used over the last decades mainly for continuous fHR monitoring during labor but also for the intermittent assessment of high-risk pregnancies in the antenatal period [2]. Al-

[5–8]. A recent systematic review and meta-analysis [9] reported a small reduction in perinatal morbidity and operative vaginal deliveries associated with the use of adjunctive ST waveform analysis. However, the method has not gained widespread acceptance mainly because ST waveform analysis remains an invasive technique; the fECG signal is recorded with a fetal scalp electrode applied only during labor after the membranes rupture, increasing thus the risk of maternal to fetal transmission of infection.

Apart from intrapartum monitoring, fHR analysis may play an important role in the ambulatory assessment of high-risk pregnancies, which is currently an area of investigation [10]. Pathological conditions such as pre-eclampsia or placental insufficiency may lead to intra-uterine growth restriction (IUGR). Fetuses suffering from IUGR due to placental insufficiency are at risk of severe complications (e.g. stillbirth and impaired neurological development); antenatal surveillance modalities aim to detect signs of progressive deterioration in these fetuses in order to accurately predict fetal risk and decide upon the optimal timing of pre-term delivery. Ultrasound, to either perform complex biophysical profile scoring evaluation or multivessel Doppler investigation, is

the method more widely used in clinical practice for this purpose [2, 11] and proven to be safe in the long-term [12]. In addition to some specific disadvantages (e.g. need for specialized bulky equipment, highly trained and experienced personnel), the main limitation of Doppler ultrasound is its sensitivity to any movement; the method can be used only in hospital settings and is unsuitable for ambulatory monitoring. Monitoring of fHR, combined with computerized analysis of ST waveform or short-term fHR variation, has also been proposed, but its use remains limited mainly due to the invasiveness of the method [2, 11].

The abdominal ECG (abdECG) recording is a very promising alternative method that could be used for fetal monitoring either during labor or in the antenatal period with several important advantages. The technique is totally non-invasive using only lightweight electrodes, can be used for long duration recordings [13], is simple to operate even by the mothers themselves and thus may be potentially suitable for ambulatory conditions and telemonitoring. However, abdECG is a composite signal consisting from both the maternal ECG (mECG) and the fECG as well as noise interference. Two major approaches

exist currently in the analysis of fECG signals recorded from the pregnant woman: a) direct extraction of the fHR from the abdECG, or b) extraction of the fECG from the abdECG and subsequent fHR identification. The extraction of fHR and fECG from abdominal recordings still remains a very complex task; various research efforts using signal processing techniques have been reported [13, 14–23]. Blind source separation (BSS) methods have also been used and shown to be more efficient in extracting several source signals from a large number of observed signals [24–27]. Lu et al. [28] recently proposed ICA with reference (ICA-R) to improve the efficiency of BSS application. However, the majority of these methods are characterized by several limitations [29].

There are only a few systems reported in the literature for fetal cardiac health monitoring based on abdECG recordings [30–33]. Jezewski et al. [30] proposed a four-lead monitoring system for the extraction of fECG, mHR, fHR, uterine contractions and T/QRS ratio, although no numerical results were presented in their study. Taylor et al. [31] used the QinetiQ fECG technology [32] to extract non-invasively fECG and fHR signals. Using a twelve-lead recording system, average fECG waveforms may be extracted without performing ST waveform analysis. Monica Healthcare Ltd. [33] developed a fetal/maternal monitoring system designed for the acquisition of mHR, fHR, maternal movements and maternal uterine activity (20 weeks of gestation until delivery), using five electrodes placed around the mother's abdomen connected to a wearable monitor. Lack of fECG morphology extraction for further waveform analysis and capability of real beat-to-beat extraction are the main disadvantages of this system.

In this work we aim to facilitate the prenatal methodology for fetal cardiac health monitoring by developing a transabdominal system for long-term monitoring using ECG leads placed on the mother's abdomen. Data analysis is carried out automatically in three stages. In the first stage, the recorded abdECG is analyzed using 3D phase-space analysis and multivariate denoising techniques, in order to extract the fHR and the eliminated ECG (eECG), i.e. the abdECG without the maternal QRS complexes. In the second stage, independent component analysis (ICA) is applied to the eECG; the extracted components

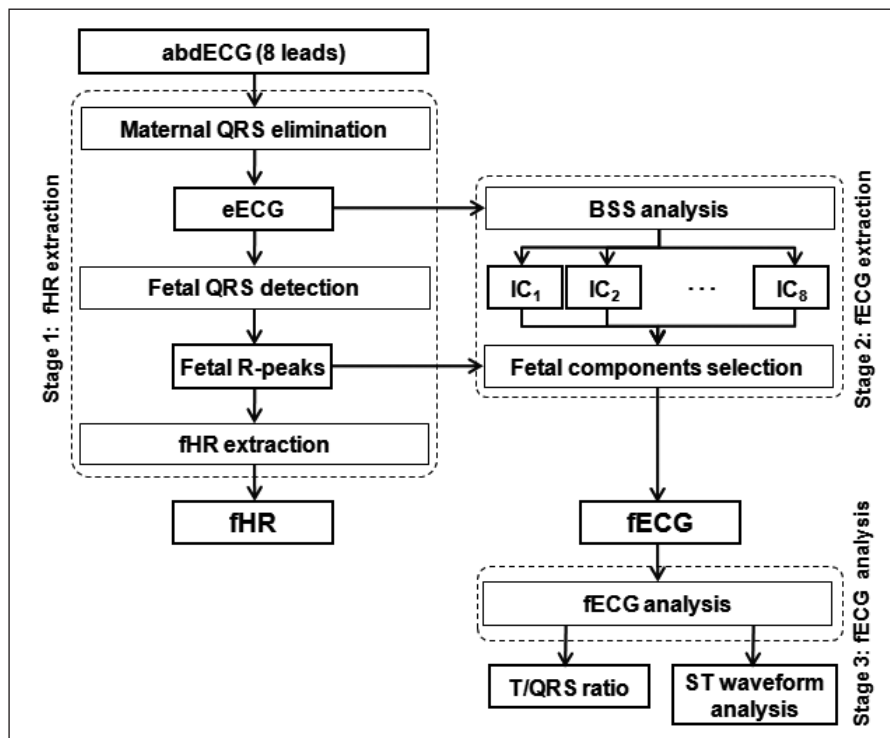


Fig. 1 Flowchart of the three-stage proposed methodology

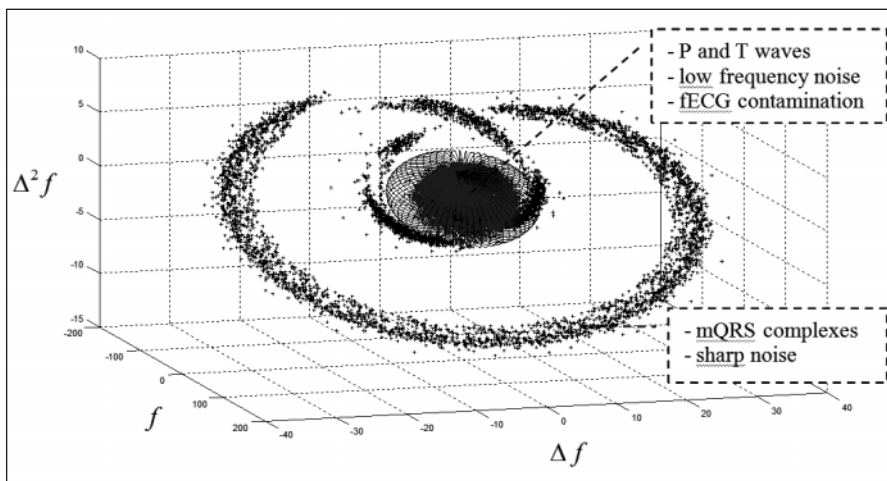


Fig. 2 The 3D phase space and the corresponding ellipsoid

( $IC_{1...N}$ , where  $N$  is the number of recorded leads) that include strong fECG interference are identified (based on the fHR obtained in the first stage) and combined, form the fECG. Finally, in the third stage, the fECG signal is processed to extract several features important for fetal monitoring. More specifically, the T/QRS ratio is calculated and the ST waveform is analyzed. The proposed method-

ology described above is then evaluated in a large number of simulated signals generated using an abdECG generator [34] and various signal-to-noise ratios (SNRs). The proposed method presents several advantages compared to previously reported methods; it is non-invasive and offers automated identification of fECG and automated ST waveform analysis employing an efficient BSS approach.

The paper is structured as follows: the three-stage methodology is described in Section 2. The datasets used to configure and evaluate the methodology are presented in Section 3, while the implementation of the methodology (i.e. the selection of the techniques used in each stage of the methodology and the procedure utilized to identify the parameters of the methodology) is presented in Section 4. Results of the evaluation of the methodology are discussed in Section 5. Discussion (Section 6) and concluding remarks (Section 7) follow.

## 2. Materials and Methods

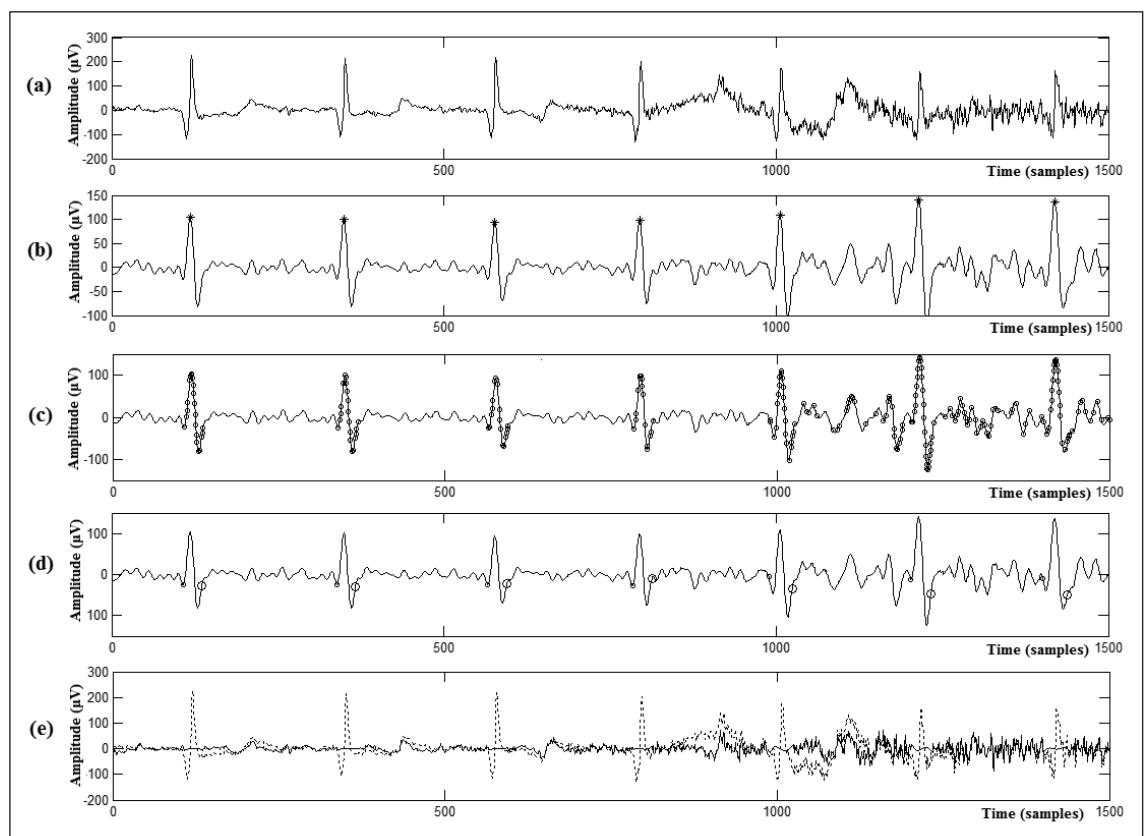
The three stages of the proposed methodology are shown in ►Figure 1 and are described in detail below.

### 2.1 Stage 1: fHR Extraction

In the first stage, the abdECG consisting of  $N$  leads (8 in our case) is analyzed to extract the eECG and fHR. The application used is based

Fig. 3

A working example of step 1 of stage 1 of the proposed methodology: a) abdECG signal, b) bandpass-filtered signal with detected mQRS time positions (with stars \*), c) detected mQRS-points (with circles ○), d) detected maternal fiducial points (with circles ○) and e) abdECG (with dotted lines ···) and eECG signals (with solid lines —), respectively.



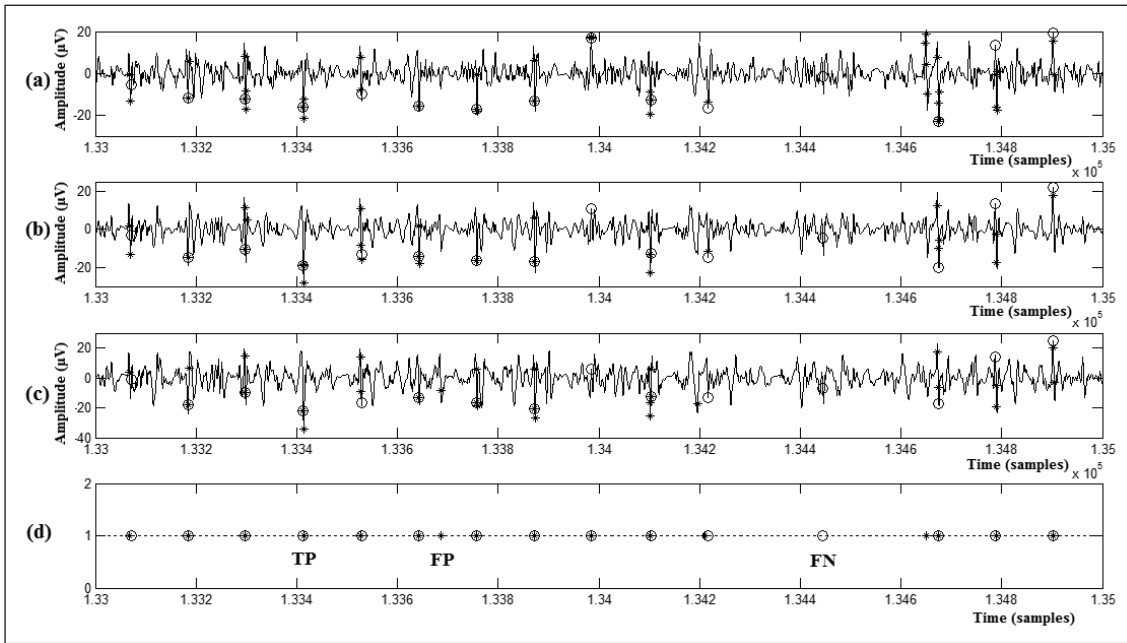


**Fig. 4** a, b, c) Fetal QRS points (denoted with circles on the signal) detected in three leads of the signal, and d) all detected points for the three leads merged in one single lead (denoted with circles ○) and the annotated fetal R peaks (with star \*) , not including fetal R-peaks which overlap with mQRSs.

on a methodology proposed by our group and described in detail previously [29]. Briefly, the first stage includes three steps [29].

### 2.1.1 Step 1: Maternal QRS Elimination

In the first step, preprocessing of the abdECG is applied. Each abdECG lead is filtered using a band-pass filter at the 4–20 Hz subband, eliminating noise artefacts from the abdECG signal. That results to the filtered signal  $f$ , represented as a  $N \times M$  matrix, where  $M$  is the number of samples. Thus, each signal (lead) is a row in the matrix. The points belonging to maternal QRSs (mQRSs) are identified from the filtered abdECG. For this purpose, initially QRS detection is performed to detect the mQRSs (using a parabolic fitting technique) [35] and then the (modified) three-dimensional (3D) phase-space analysis [36, 37] is used to detect the points belonging to the mQRS complexes. The above is applied into the first lead of the signal  $f$ .

The 3D phase-space plot, based on 3D Poincaré maps, is created after calculation of the first ( $\Delta f$ ) and the second ( $\Delta^2 f$ ) derivatives of the first row of the signal  $f$  and then plotting of each point  $(f(i), \Delta f(i), \Delta^2 f(i))$  where  $i$  is the time sample. A 3D ellipsoid is defined, using the universal criterion  $\lambda_F$  [36]. After application of the 3D phase-space plot to ECG data (► Fig. 2), the points in the large surrounding torus mainly correspond to the mQRS complexes (points of interest) and sharp noise contamination [34], while the points in the middle correspond mainly to P and T waves, low frequency noise activity and fECG contamination.

In contrary to the initial approach [36], which assumes that the samples of the signal are normally distributed, in the case of ECG this assumption does not hold. Thus, we have introduced three parameters,  $a_1$ ,  $b_1$ , and  $c_1$ , which multiply  $\lambda_{\sigma_f}$ ,  $\lambda_{\sigma_{\Delta f}}$  and  $\lambda_{\sigma_{\Delta^2 f}}$ , respectively. The above described approach is a generalization of the method proposed in [36]. Based on this, the procedure for mQRS detection by the phase-space analysis is summarized as follows:

1. Set  $f$  to be of zero mean:  $f = f - \frac{1}{N} \sum_{i=1}^N f(i)$ .
2. Calculate the derivatives  $\Delta f$  and  $\Delta^2 f$ :  
 $\Delta f(i) = (f(i+1) - f(i-1))/2$  and  
 $\Delta^2 f(i) = (f(i+2) - f(i-2) - 2f(i))/4$
3. Calculate the angle  $\theta$ :  
 $\theta = \tan^{-1}((f \cdot \Delta^2 f^T)/(f \cdot f^T))$ .
4. Rotate data:  

$$\begin{bmatrix} f^T & \Delta f^T & \Delta^2 f^T \end{bmatrix} = \begin{bmatrix} f^T & \Delta f^T & \Delta^2 f^T \end{bmatrix} \begin{bmatrix} \cos \theta & 0 & -\sin \theta \\ 0 & 1 & 0 \\ \sin \theta & 0 & \cos \theta \end{bmatrix}$$
5. Calculate  $\lambda$ :  $\lambda = \sqrt{2 \ln N}$ .
6. Calculate the standard deviation  $\sigma_f$ ,  $\sigma_{\Delta f}$  and  $\sigma_{\Delta^2 f}$  of all three variables  $f$ ,  $\Delta f$  and  $\Delta^2 f$ .

$$threshold = \frac{1}{N} \sum_{i=1}^N cor(IC_i, fHR) + \frac{1}{N} \sum_{j=1}^N \left| cor(IC_j, fHR) - \frac{1}{N} \sum_{i=1}^N cor(IC_i, fHR) \right|$$

**If**  $cor(IC_i, fHR) > threshold$

**then**

$IC_i$  contains strong fetal interference ( $fIC_i$ )

**Fig. 5** Rule identifying the fetal ICs

7. Calculate the expected maxima  $\lambda\sigma_f$ ,  $\lambda\sigma_{\Delta f}$  and  $\lambda\sigma_{\Delta^2 f}$ .

$$\frac{f(i)^2}{(a_1\lambda\sigma_f)^2} + \frac{\Delta f(i)^2}{(b_1\lambda\sigma_{\Delta f})^2} + \frac{\Delta^2 f(i)^2}{(c_1\lambda\sigma_{\Delta^2 f})^2} > 1$$

8. Considering an ellipsoid with principal axes  $a_1\lambda\sigma_f$ ,  $b_1\lambda\sigma_{\Delta f}$  and  $c_1\lambda\sigma_{\Delta^2 f}$ , a point  $(f(i), \Delta f(i), \Delta^2 f(i))$  is an outlier (i.e. lies outside this ellipsoid) if:

Each outlier is replaced using spline interpolation.

9. The above steps are applied iteratively until no outliers are identified in step 8.

In our case, we have defined the values of the parameters to be  $a_1 = b_1 = 1$  and  $c_1 = 0.8$ ; the procedure that was followed for defining these values is described in the Results sec-

Fig. 6

The ICs after application of EFICA in eECG signals. Solid lines indicate the positions of annotated fetal R peaks while the circles  $\circ$  indicate the detected IC peaks. Numbers on the right ('04', '00'...'05') correspond to the number of true positive R peaks and the stars \* indicate the channels of detected fICs.

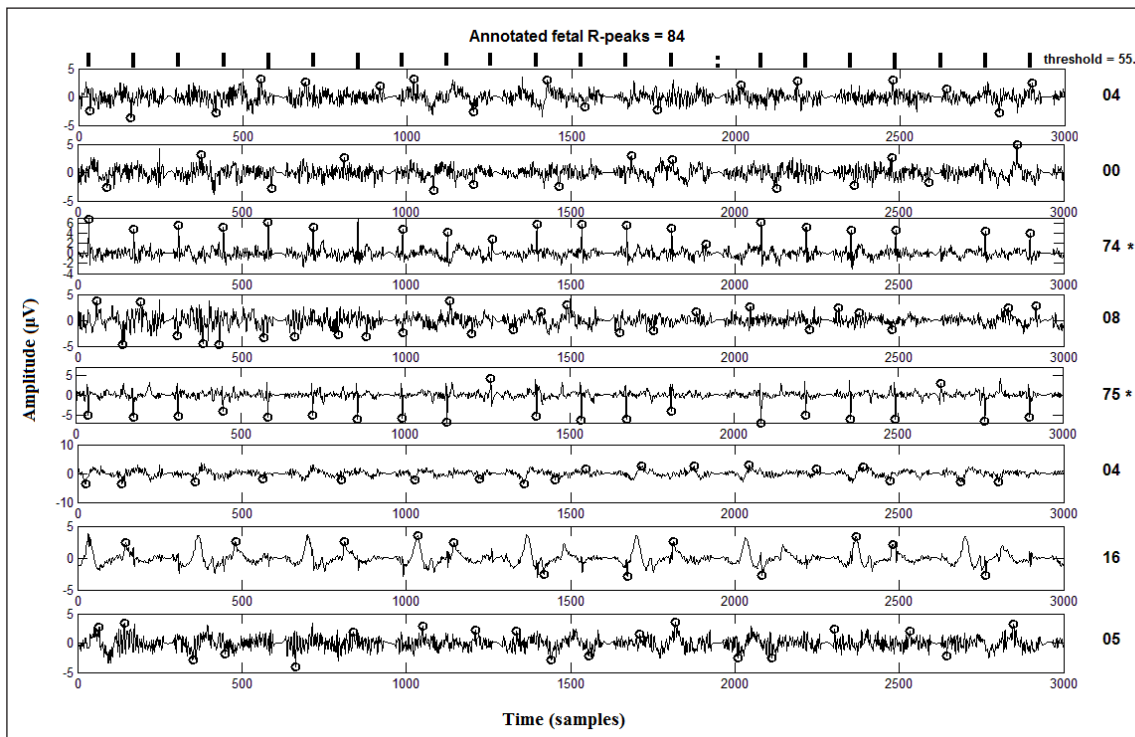
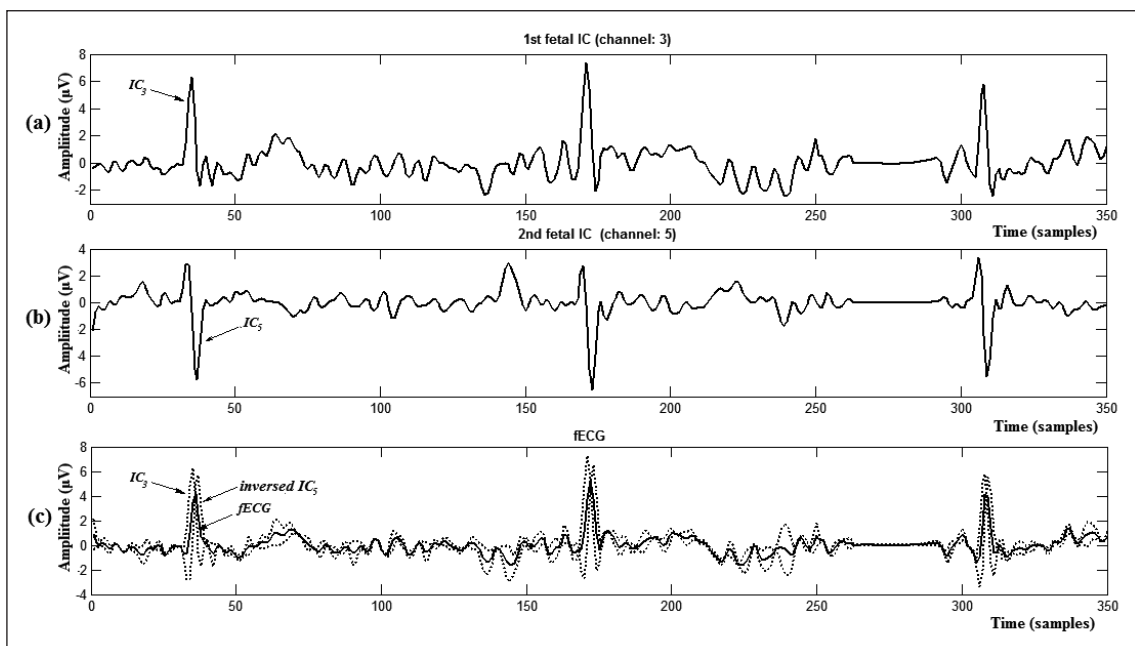
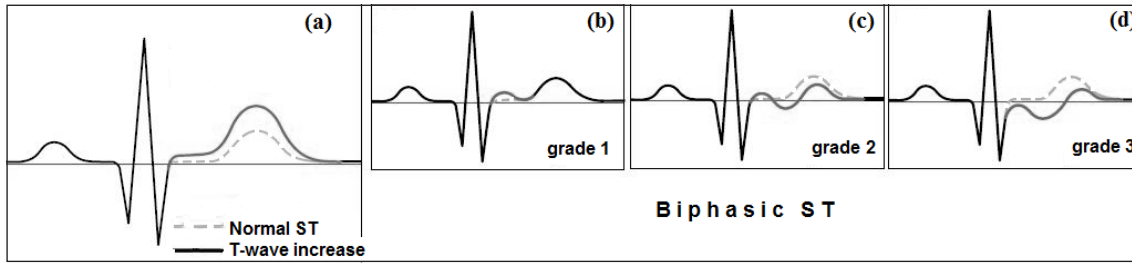


Fig. 7

A working example of the merging procedure: a) the first fIC (corresponding to channel 3 -  $fIC_3$ ), b) the second fIC (corresponding to channel 5 -  $fIC_5$ ), and c) the fECG signal. Dotted lines correspond to the  $fIC_3$  and inverted  $fIC_5$ .





**Fig. 8** ST waveform classification [1]: a) Normal ST, b) biphasic ST of grade 1, c) biphasic ST of grade 2, and d) biphasic ST of grade 3

tion. A 3D phase space map and the corresponding ellipsoid are shown in ►Figure 2.

For each maternal R peak, the last consecutive mQRS points to the left and right define the maternal Q wave start (mQRS onset) and S wave end (mQRS offset), respectively. Then, spline interpolation (using higher-order polynomial curve fitting) is accomplished between the fiducial points and elimination from the initial abdECG signal (not the filtered) is performed. The elimination procedure is applied in all abdECG leads, thus resulting to the eECG. A working example of step 1 is presented in ►Figure 3.

### 2.1.2 Step 2: Fetal QRS Detection

The second step locates the candidate fetal R peaks. Each lead of the eECG (generated from the previous step) is denoised using sequentially: i) band-pass filtering in the 4–80 Hz subband [38] and ii) a multivariate denoising procedure [39]. The denoised eECG is used to detect the fetal R peaks which do not overlap with mQRSs. The 3D phase space thresholding is applied in each lead of the denoised eECG, thus detecting all spikes which are candidate fetal R peaks. We employ  $a_2 = 1.0$ ,  $b_2 = 1.4$  and  $c_2 = 1.5$  [29]. This procedure results to eight sets of points (one for each lead) which are merged into a single set of points. The outcome of step 2 is the fetal R peaks not overlapping with the mQRSs (eliminated in step 1) and a working example is presented in ►Figure 4.

### 2.1.3 Step 3: fHR Extraction

In the third step, the fetal R peaks which overlap with the maternal QRS complexes are detected, using a histogram-based technique [20, 29]. The results from step 2 (fetal R peaks not overlapping with the mQRSs) and those from step 3 (fetal R peaks overlapping with the mQRSs) are combined to form the fetal R-R interval signal and subsequently the fHR is extracted.

### 2.2 Stage 2: fECG Extraction

In this stage, the fECG is extracted from the eECG. The eECG, extracted from the abdECG in the first stage, is analyzed using the EFICA (Efficient Variant of FastICA) [40, 41], an improved version of FastICA algorithm, and the result is eight independent components ( $IC_1 - IC_8$ ). EFICA suffers from the permutation problem, i.e. the independent components (ICs) that contain fECG interference (usually of 1 or 2 channels depending of the SNR) are not predefined and must be identified in the resulted ICs. Thus, a QRS detection algorithm [35] is applied in each IC, in order to detect the signal's peaks (IC peaks). The only modification of the parabolic fitting approach for the fQRS detection is a reduction of the width of the fitting window. This procedure results to one set of points for each lead which is then correlated with the fHR (already extracted in stage 1). Thus, one value for each IC is obtained, which

corresponds to the correlation between the current IC and the fHR. Based on the correlation values, the average correlation and the standard deviation are calculated. The ICs which contain strong fetal interference, called fetal ICs (fICs), are identified by the following simple rule shown in ►Figure 5, where  $cor(a, b)$  is the correlation measure between  $a$  and  $b$ . The correlation is defined as the number of true positive fetal R peaks, i.e. the number of IC peaks which correspond to fetal R peaks. An IC peak is considered as true positive if it lies in a 20-point time window centered in a fetal R peak; The width of the window is set to 20 points since the maximum fQRS duration is approximately 65 msec, which corresponds to 20 sample points for sampling rate 300 Hz [42, 43]. A working example of the above procedure (the IC generated from the EFICA analysis and the fICs identification) is shown in ►Figure 6.

After fICs identification, those with negative polarity (such as the 5th channel of the 8 ICs in ►Fig. 6) are inverted (i.e. are set with positive polarity) and then the fECG signal is estimated as the average of all detected fICs. In ►Figure 6, channels 3 and 5 (mentioned with stars “\*”) are located as the fICs, after the analysis described above. The fECG is estimated as:

$$fECG(t) = \frac{1}{M} \sum_{i=1}^M fIC_i(t),$$

where  $M$  is the number of the available fICs and  $t$  is a time instant. An example of the merging procedure is shown in ►Figure 7.

### 2.3 Stage 3: fECG Analysis

The fECG extracted in stage 2 is further processed for T/QRS estimation and ST segment analysis. For each fetal R peak ( $fR$ ), an average fetal PQRST complex ( $fPQRST$ ) is created

```

if  $ST_{area} \leq 0.2 \cdot ST_{|area|}$  then biphasic of grade 3

else_if  $ST_{area} < 0.8 \cdot ST_{|area|}$  then biphasic of grade 2

else normal
    
```

**Fig. 9** Rule for classification of the ST waveform

from the previous 30 *fPQRST* complexes. Typical time intervals of the fECG waveforms were extracted from previous studies [42, 43].

The length of each average *fPQRST* complex is equal to 330 msec which corresponds to a window of 100 samples [(*fRi* - 100) msec - (*fRi* + 230) msec], where *fRi* is the *i*th *fR*. Initially, for accurate ST analysis of the average *fPQRST* complex, precise identification of the isoelectric line is required. The isoelectric line is defined as:

$$isoelectric = \frac{1}{21} \sum_{t=fR_i-45}^{fR_i-15} fPQRST(t).$$

and is subtracted from the average *fPQRST* complex.

Accurate measurements of changes in T wave amplitude are represented as the ratio between the amplitude of the T wave and the QRS complex (T/QRS ratio). The QRS amplitude is calculated as:

$$QRS_{amp} = \max_{t \in [fR_i-10, fR_i+10]} fTQRST(t) - \min_{t \in [fR_i-10, fR_i+10]} fTQRST(t),$$

while the T wave peak is estimated as:

$$T_{amp} = \max_{t \in [fR_i+35, fR_i+200]} fTQRST(t).$$

The ST waveform of each average *fPQRST* complex is analyzed and characterized as normal ST or biphasic ST of grade 1, 2 or 3. Examples of the ST waveforms are presented in ► Figure 8.

A horizontal or upward leaning, positive ST segment and a T wave amplitude which is stable and does not increase, define a normal ST. An increase in T wave amplitude is the typical fetal reaction to hypoxia [1, 8]; this pattern implies that the fetal metabolic defense is intact and the fetus is able to handle hypoxia. A biphasic ST is defined as a downward-leaning ST segment. This pattern occurs if the fetal heart is either exposed to hypoxia and is not able to respond or has a reduced capacity to respond because of previous exposure to stress situations. Biphasic STs are classified in three categories: grade 1 is a downward-leaning ST segment with the entire segment above the baseline, grade 2 when a component of the ST segment crosses the baseline and grade 3 when the whole of ST segment is below the baseline. A significant biphasic event occurs when there are more

**Table 1** Obtained cross-correlation results between the initial fECG signals and the fECG signal using abdECG and eECG signals

| Signals | Signal (SNR dB)<br>Cross-correlation Results (max) |       |       |       |       |       | Mean         |
|---------|--|-------|-------|-------|-------|-------|--------------|
|         | -5   | -2    | 0     | +2    | +5    | +10   |              |
| abdECG  | 0.252  | 0.234 | 0.261 | 0.326 | 0.639 | 0.777 | <b>0.415</b> |
| eECG    | 0.634  | 0.682 | 0.683 | 0.742 | 0.871 | 0.903 | <b>0.753</b> |

**Table 2** Obtained results for fECG correlation and T/QRS ratio for all BSS analysis techniques. The combinatory index is shown in the last column

|                        | Correlation      | Initial T/QRS ratio = 0.1523 |                   |
|------------------------|------------------|------------------------------|-------------------|
| BSS analysis technique | fECG correlation | Mean T/QRS ratio             | Combinatory index |
| AMUSE                  | 0.463            | 0.088                        | 0.522             |
| SOBI                   | 0.491            | 0.093                        | 0.551             |
| SOBI-PBF               | 0.616            | 0.145                        | 0.784             |
| WASOBI                 | 0.564            | 0.106                        | 0.632             |
| EWASOBI                | 0.589            | 0.108                        | 0.649             |
| FJADE                  | 0.758            | 0.210                        | 0.689             |
| JADEop                 | 0.763            | 0.212                        | 0.686             |
| QJADE                  | 0.775            | 0.241                        | 0.597             |
| FAJDC4                 | 0.683            | 0.169                        | 0.787             |
| FPICA                  | 0.734            | 0.204                        | 0.699             |
| POWERICA               | 0.662            | 0.166                        | 0.788             |
| EFICA                  | <b>0.695</b>     | <b>0.156</b>                 | <b>0.835</b>      |
| COMBI                  | 0.688            | 0.172                        | 0.781             |
| MULCOMBI               | 0.677            | 0.165                        | 0.797             |
| SANG                   | 0.685            | 0.161                        | 0.815             |
| NG-FICA                | 0.677            | 0.160                        | 0.813             |
| <b>Average</b>         | <b>= 0.658</b>   | <b>= 0.160</b>               | <b>0.714</b>      |

**Table 3** Obtained results from the application of the fHR extraction step to the simulated signals using (*a*<sub>2</sub>, *b*<sub>2</sub>, *c*<sub>2</sub>) = (1.0, 1.4, 1.5)

| Signals      | Results     |            |            |              |              |              |
|--------------|-------------|------------|------------|--------------|--------------|--------------|
|              | SNR (dB)    | TP         | FP         | FN           | Se (%)       | PDV (%)      |
| -5           | 561         | 105        | 90         | 86.18        | 84.23        | 74.21        |
| -2           | 643         | 11         | 8          | 98.77        | 98.32        | 97.13        |
| 0            | 648         | 5          | 3          | 99.54        | 99.23        | 98.78        |
| 2            | 648         | 4          | 3          | 99.54        | 99.39        | 98.93        |
| 5            | 650         | 1          | 1          | 99.85        | 99.85        | 99.69        |
| 10           | 651         | 0          | 0          | 100          | 100          | 100          |
| <b>Total</b> | <b>3801</b> | <b>126</b> | <b>105</b> | <b>97.31</b> | <b>96.84</b> | <b>94.79</b> |

**Table 4** Obtained correlation results between the fECG in all different SNRs, with the eight channels of the fECG, generated from the simulator for: a) series 2, b) series 3, c) series 4, and d) series 5 of abdECG recordings

| a) 2 <sup>nd</sup> abdECG series – normal ST waveform                              |                              |        |        |        |        |        |        |        |              |
|--|------------------------------|--------|--------|--------|--------|--------|--------|--------|--------------|
| Signals  | normalized cross-correlation |        |        |        |        |        |        |        |              |
| SNR (dB)   | Ch. 1                        | Ch. 2  | Ch. 3  | Ch. 4  | Ch. 5  | Ch. 6  | Ch. 7  | Ch. 8  | mean         |
| -5   | 0.753                        | 0.694  | 0.617  | 0.684  | 0.276  | 0.378  | 0.713  | 0.715  | <b>0.604</b> |
| -2   | 0.786                        | 0.708  | 0.66   | 0.685  | 0.317  | 0.436  | 0.775  | 0.758  | <b>0.641</b> |
| 0  | 0.845                        | 0.777  | 0.721  | 0.724  | 0.356  | 0.48   | 0.827  | 0.807  | <b>0.692</b> |
| 2  | 0.902                        | 0.834  | 0.753  | 0.8    | 0.34   | 0.474  | 0.862  | 0.856  | <b>0.728</b> |
| 5  | 0.906                        | 0.824  | 0.771  | 0.78   | 0.375  | 0.513  | 0.893  | 0.87   | <b>0.742</b> |
| 10   | 0.979                        | 0.91   | 0.826  | 0.863  | 0.383  | 0.527  | 0.938  | 0.928  | <b>0.794</b> |
| b) 3 <sup>rd</sup> abdECG series – normal and biphasic (grade 2) ST waveforms      |                              |        |        |        |        |        |        |        |              |
| Signals  | normalized cross-correlation |        |        |        |        |        |        |        |              |
| SNR (dB)   | Ch. 1                        | Ch. 2  | Ch. 3  | Ch. 4  | Ch. 5  | Ch. 6  | Ch. 7  | Ch. 8  | mean         |
| -5   | 0.599                        | 0.57   | 0.538  | 0.524  | 0.283  | 0.375  | 0.609  | 0.57   | <b>0.509</b> |
| -2   | 0.703                        | 0.652  | 0.61   | 0.593  | 0.285  | 0.397  | 0.702  | 0.661  | <b>0.575</b> |
| 0  | 0.81                         | 0.765  | 0.69   | 0.706  | 0.291  | 0.42   | 0.783  | 0.751  | <b>0.652</b> |
| 2  | 0.871                        | 0.832  | 0.762  | 0.743  | 0.346  | 0.482  | 0.853  | 0.807  | <b>0.712</b> |
| 5  | 0.882                        | 0.844  | 0.772  | 0.756  | 0.352  | 0.49   | 0.862  | 0.818  | <b>0.722</b> |
| 10   | 0.936                        | 0.902  | 0.819  | 0.812  | 0.371  | 0.515  | 0.907  | 0.867  | <b>0.766</b> |
| c) 4 <sup>th</sup> abdECG series – normal and biphasic (grade 3) ST waveforms      |                              |        |        |        |        |        |        |        |              |
| Signals  | normalized cross-correlation |        |        |        |        |        |        |        |              |
| SNR (dB)   | Ch. 1                        | Ch. 2  | Ch. 3  | Ch. 4  | Ch. 5  | Ch. 6  | Ch. 7  | Ch. 8  | mean         |
| -5   | 0.516                        | 0.63   | 0.621  | 0.421  | 0.429  | 0.493  | 0.521  | 0.444  | <b>0.509</b> |
| -2   | 0.572                        | 0.671  | 0.67   | 0.467  | 0.447  | 0.526  | 0.586  | 0.504  | <b>0.555</b> |
| 0  | 0.594                        | 0.717  | 0.718  | 0.482  | 0.484  | 0.568  | 0.607  | 0.513  | <b>0.585</b> |
| 2  | 0.624                        | 0.759  | 0.734  | 0.53   | 0.48   | 0.56   | 0.615  | 0.536  | <b>0.605</b> |
| 5  | 0.681                        | 0.82   | 0.806  | 0.571  | 0.528  | 0.622  | 0.683  | 0.589  | <b>0.663</b> |
| 10   | 0.719                        | 0.844  | 0.85   | 0.581  | 0.568  | 0.67   | 0.742  | 0.632  | <b>0.701</b> |
| d) 5 <sup>th</sup> abdECG series – normal and biphasic (grades 2 & 3) ST waveforms |                              |        |        |        |        |        |        |        |              |
| Signals  | normalized cross-correlation |        |        |        |        |        |        |        |              |
| SNR (dB)   | Ch. 1                        | Ch. 2  | Ch. 3  | Ch. 4  | Ch. 5  | Ch. 6  | Ch. 7  | Ch. 8  | mean         |
| -5   | 0.557                        | 0.6223 | 0.5823 | 0.435  | 0.3318 | 0.3844 | 0.5343 | 0.523  | <b>0.496</b> |
| -2   | 0.569                        | 0.6625 | 0.6696 | 0.6774 | 0.3948 | 0.3886 | 0.6434 | 0.6325 | <b>0.580</b> |
| 0  | 0.782                        | 0.7516 | 0.6894 | 0.7308 | 0.4698 | 0.4037 | 0.6683 | 0.6512 | <b>0.643</b> |
| 2  | 0.858                        | 0.8879 | 0.7877 | 0.753  | 0.4764 | 0.4567 | 0.6904 | 0.7174 | <b>0.703</b> |
| 5  | 0.896                        | 0.8903 | 0.8237 | 0.7862 | 0.4948 | 0.5833 | 0.7892 | 0.7678 | <b>0.754</b> |
| 10   | 0.900                        | 0.8922 | 0.8366 | 0.7962 | 0.499  | 0.6179 | 0.8878 | 0.7804 | <b>0.776</b> |

than two consecutive biphasic ECG complexes. With the progression of disturbance in myocardial function, a shift from biphasic grade 1 to grades 2 and 3 might be observed [1].

The classification of the ST waveform is based on the ST area:

$$ST_{area} = \sum_{t=fR_i+15}^{fR_i+80} fTQRST(t)$$

and the ST absolute area:

$$ST_{|area|} = \sum_{t=fR_i+15}^{fR_i+80} |fTQRST(t)|,$$

as can be seen in ► Figure 9.

Although three different grades of biphasic ST exist, grade 1 is considered as normal (i.e. not related to a cardiac disorder [1, 8]) and thus, we mainly focus on the grade 2 and 3 categories of the biphasic ST waveforms, while all remaining ST waveforms are considered as normal.

### 3. Dataset

The validation of the proposed methodology is based on simulated abdECG signals generated using a three-dimensional dynamic model of the electrical activity of the heart; this model considers the fetus to be in its normal vertex position with its head down and its face towards the right arm of the mother [34]. The signals are generated from a linear model which accounts for the temporal movements and rotations of the cardiac dipole, along with an ECG noise model. The model is specialized to maternal and fetal ECG mixtures, recorded from the thorax and abdomen of pregnant women. Our methodology is based on the analysis of abdominal signals only, and therefore thorax signals are excluded. A specific number and positioning of the leads is employed. The number of signal leads was set to 8 in our methodology, as it has been shown that BSS methods require as many external sensors as possible (up to 8) in order to perfectly recover the original signal sources [24–26, 44], while sensors must also record “different mixtures” [44]. The lead positions proposed are shown in ► Figure 10, and are based on the map of fetal signal strength over the mother’s abdomen that has been previously reported [31, 32] and the fact that the fetus’ usual position is the normal

**Table 5**

Obtained results for the T/QRS ratio calculated from the extracted fECG (final T/QRS ratio) and the T/QRS ratio calculated from the initial simulated fECG (initial T/QRS ratio), for: a) series 2, b) series 3, c) series 4, and d) series 5 of abdECG recordings

| <b>a) abdECG series 2 – normal ST waveform</b>                                |              |              |              |              |              |              |              |              |              |               |              |
|---|--------------|--------------|--------------|--------------|--------------|--------------|--------------|--------------|--------------|---------------|--------------|
| <b>Signals Final T/QRS ratio (Initial T/QRS ratio: 0.152)</b>                 |              |              |              |              |              |              |              |              |              |               |              |
| <b>SNR (dB)</b>   | <b>Run 1</b> | <b>Run 2</b> | <b>Run 3</b> | <b>Run 4</b> | <b>Run 5</b> | <b>Run 6</b> | <b>Run 7</b> | <b>Run 8</b> | <b>Run 9</b> | <b>Run 10</b> | <b>Mean</b>  |
| -5  | 0.142        | 0.150        | 0.134        | 0.142        | 0.152        | 0.136        | 0.149        | 0.172        | 0.138        | 0.162         | <b>0.148</b> |
| -2  | 0.120        | 0.162        | 0.150        | 0.157        | 0.165        | 0.139        | 0.139        | 0.158        | 0.157        | 0.142         | <b>0.149</b> |
| 0   | 0.163        | 0.165        | 0.164        | 0.142        | 0.158        | 0.146        | 0.153        | 0.161        | 0.170        | 0.138         | <b>0.156</b> |
| 2   | 0.142        | 0.168        | 0.165        | 0.159        | 0.156        | 0.161        | 0.134        | 0.154        | 0.164        | 0.148         | <b>0.155</b> |
| 5   | 0.156        | 0.141        | 0.151        | 0.151        | 0.145        | 0.147        | 0.156        | 0.143        | 0.145        | 0.160         | <b>0.150</b> |
| 10  | 0.179        | 0.163        | 0.131        | 0.163        | 0.165        | 0.151        | 0.158        | 0.157        | 0.140        | 0.141         | <b>0.155</b> |
| <b>Mean final T/QRS ratio:</b>  |              |              |              |              |              |              |              |              |              |               | <b>0.152</b> |
| <b>b) abdECG series 3 – normal and biphasic (grade 2) ST waveforms</b>        |              |              |              |              |              |              |              |              |              |               |              |
| <b>Signals Final T/QRS ratio (Initial T/QRS ratio: 0.113)</b>                 |              |              |              |              |              |              |              |              |              |               |              |
| <b>SNR (dB)</b>   | <b>Run 1</b> | <b>Run 2</b> | <b>Run 3</b> | <b>Run 4</b> | <b>Run 5</b> | <b>Run 6</b> | <b>Run 7</b> | <b>Run 8</b> | <b>Run 9</b> | <b>Run 10</b> | <b>Mean</b>  |
| -5  | 0.163        | 0.103        | 0.137        | 0.142        | 0.116        | 0.059        | 0.107        | 0.097        | 0.131        | 0.105         | <b>0.116</b> |
| -2  | 0.100        | 0.128        | 0.018        | 0.145        | 0.125        | 0.130        | 0.127        | 0.126        | 0.136        | 0.136         | <b>0.117</b> |
| 0   | 0.110        | 0.131        | 0.121        | 0.103        | 0.117        | 0.145        | 0.108        | 0.097        | 0.116        | 0.114         | <b>0.116</b> |
| 2   | 0.119        | 0.099        | 0.138        | 0.126        | 0.162        | 0.137        | 0.111        | 0.102        | 0.121        | 0.121         | <b>0.124</b> |
| 5   | 0.130        | 0.118        | 0.113        | 0.110        | 0.128        | 0.118        | 0.127        | 0.127        | 0.101        | 0.111         | <b>0.118</b> |
| 10  | 0.121        | 0.126        | 0.124        | 0.120        | 0.111        | 0.125        | 0.118        | 0.122        | 0.123        | 0.120         | <b>0.121</b> |
| <b>Mean final T/QRS ratio:</b>  |              |              |              |              |              |              |              |              |              |               | <b>0.119</b> |
| <b>c) abdECG series 4 – normal and biphasic (grade 3) ST waveforms</b>        |              |              |              |              |              |              |              |              |              |               |              |
| <b>Signals Final T/QRS ratio (Initial T/QRS ratio: 0.088)</b>                 |              |              |              |              |              |              |              |              |              |               |              |
| <b>SNR (dB)</b>   | <b>Run 1</b> | <b>Run 2</b> | <b>Run 3</b> | <b>Run 4</b> | <b>Run 5</b> | <b>Run 6</b> | <b>Run 7</b> | <b>Run 8</b> | <b>Run 9</b> | <b>Run 10</b> | <b>Mean</b>  |
| -5  | 0.094        | 0.122        | 0.203        | 0.137        | 0.154        | 0.139        | 0.134        | 0.123        | 0.135        | 0.106         | <b>0.135</b> |
| -2  | 0.153        | 0.127        | 0.129        | 0.174        | 0.125        | 0.123        | 0.121        | 0.131        | 0.129        | 0.130         | <b>0.134</b> |
| 0   | 0.106        | 0.095        | 0.116        | 0.085        | 0.093        | 0.083        | 0.093        | 0.088        | 0.096        | 0.126         | <b>0.098</b> |
| 2   | 0.105        | 0.093        | 0.084        | 0.101        | 0.074        | 0.088        | 0.093        | 0.080        | 0.095        | 0.093         | <b>0.091</b> |
| 5   | 0.167        | 0.134        | 0.126        | 0.076        | 0.071        | 0.082        | 0.067        | 0.089        | 0.093        | 0.076         | <b>0.098</b> |
| 10  | 0.102        | 0.114        | 0.136        | 0.051        | 0.072        | 0.075        | 0.064        | 0.061        | 0.064        | 0.086         | <b>0.082</b> |
| <b>Mean final T/QRS ratio:</b>  |              |              |              |              |              |              |              |              |              |               | <b>0.106</b> |
| <b>d) abdECG series 5 – normal and biphasic (grades 2 and 3) ST waveforms</b> |              |              |              |              |              |              |              |              |              |               |              |
| <b>Signals Final T/QRS ratio (Initial T/QRS ratio: 0.115)</b>                 |              |              |              |              |              |              |              |              |              |               |              |
| <b>SNR (dB)</b>   | <b>Run 1</b> | <b>Run 2</b> | <b>Run 3</b> | <b>Run 4</b> | <b>Run 5</b> | <b>Run 6</b> | <b>Run 7</b> | <b>Run 8</b> | <b>Run 9</b> | <b>Run 10</b> | <b>Mean</b>  |
| -5  | 0.143        | 0.104        | 0.112        | 0.155        | 0.148        | 0.150        | 0.111        | 0.135        | 0.089        | 0.170         | <b>0.132</b> |
| -2  | 0.166        | 0.104        | 0.103        | 0.130        | 0.132        | 0.093        | 0.152        | 0.139        | 0.162        | 0.120         | <b>0.130</b> |
| 0   | 0.148        | 0.130        | 0.154        | 0.136        | 0.163        | 0.088        | 0.132        | 0.109        | 0.142        | 0.095         | <b>0.129</b> |
| 2   | 0.126        | 0.094        | 0.164        | 0.112        | 0.148        | 0.128        | 0.082        | 0.096        | 0.121        | 0.129         | <b>0.120</b> |
| 5   | 0.160        | 0.156        | 0.099        | 0.133        | 0.115        | 0.164        | 0.095        | 0.104        | 0.101        | 0.088         | <b>0.122</b> |
| 10  | 0.104        | 0.093        | 0.103        | 0.123        | 0.106        | 0.086        | 0.123        | 0.128        | 0.148        | 0.155         | <b>0.117</b> |
| <b>Mean final T/QRS ratio:</b>  |              |              |              |              |              |              |              |              |              |               | <b>0.125</b> |

**Table 6** Classification results for ST waveform analysis, for all different SNRs cases

| Signals         |                | Results     |            |              |              |
|-----------------|----------------|-------------|------------|--------------|--------------|
| Signal (SNR dB) | ST analysis    | TP          | FN         | Se (%)       | Acc (%)      |
| -5              | Normal         | 155         | 80         | 65.96        | 68.82        |
|                 | Grade 2        | 126         | 74         | 63.00        |              |
|                 | Grade 3        | 156         | 44         | 78.00        |              |
| -2              | Normal         | 169         | 66         | 71.91        | 73.07        |
|                 | Grade 2        | 133         | 67         | 66.50        |              |
|                 | Grade 3        | 162         | 38         | 81.00        |              |
| 0               | Normal         | 179         | 56         | 76.17        | 77.95        |
|                 | Grade 2        | 144         | 56         | 72.00        |              |
|                 | Grade 3        | 172         | 28         | 86.00        |              |
| 2               | Normal         | 183         | 52         | 77.87        | 80.63        |
|                 | Grade 2        | 150         | 50         | 75.00        |              |
|                 | Grade 3        | 179         | 21         | 89.50        |              |
| 5               | Normal         | 201         | 34         | 85.53        | 86.93        |
|                 | Grade 2        | 163         | 37         | 81.50        |              |
|                 | Grade 3        | 188         | 12         | 94.00        |              |
| 10              | Normal         | 208         | 27         | 88.51        | 90.71        |
|                 | Grade 2        | 179         | 21         | 89.50        |              |
|                 | Grade 3        | 189         | 11         | 94.50        |              |
| <b>Total</b>    | <b>Normal</b>  | <b>1095</b> | <b>315</b> | <b>77.66</b> | <b>79.87</b> |
|                 | <b>Grade 2</b> | <b>902</b>  | <b>298</b> | <b>74.58</b> |              |
|                 | <b>Grade 3</b> | <b>1046</b> | <b>154</b> | <b>87.17</b> |              |

vertex position described above [34]. Based on our preliminary tests on the simulated signals, it was found that the use of eight sensors in the specific locations described above was the minimum number that could be used in order to provide optimal extraction data that would allow further analysis. The use of more sensors did not appear to improve our results, while it also increased the complexity of the data acquisition and analysis.

We employed various SNRs in the simulated abdECGs: -5, -2, 0, 2, 5 and 10 dB were used. Five series of simulated multichannel abdECG signals were generated, each of them including six signals (one for each different SNR) of eight channels (corresponding to the eight abdominal leads), with sampling frequency 300 Hz:

- Series 1: Normal ST waveforms (used for parameter calculation).

- Series 2: Normal ST waveforms.
- Series 3: Normal and biphasic (grade 2) ST waveforms.
- Series 4: Normal and biphasic (grade 3) ST waveforms.

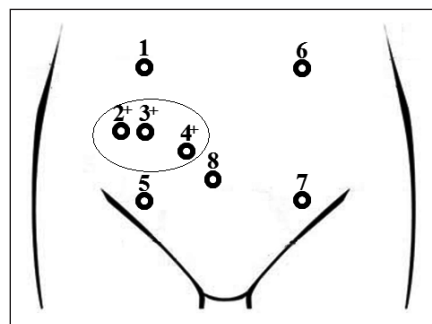


**Fig. 10** The eight leads of the simulated signals. The leads 1 and 5–8 correspond to the initial leads positioning, while 2+ to 4+ to the added leads proposed in our methodology.

- Series 5: Normal and biphasic (grade 2 and 3) ST waveforms.

The first series is used to define the values of the  $a$ ,  $b$  and  $c$  parameters in both maternal QRS elimination and fetal QRS detection steps of the first stage, while all others for the evaluation of our methodology. The simulator creates abdECGs with normal ST waveforms; the signals of the second series are then processed to create appropriate biphasic ST waveforms, generating series 3–5. Therefore, the signals included in series 2–5 are similar, having differences only in the ST waveforms.

## 4. Implementation

As mentioned in the Introduction section, several BSS techniques have been widely proposed for the extraction of fECG from multichannel signals of the pregnant woman [25, 26, 45]. However, all these BSS approaches have been applied in the multichannel signals of abdomen and/or thorax without providing any preprocessing step, contrary to our methodology. ▶ Table 1 presents the results of normalized cross-correlation between the initial fECG signals and the fECG extracted using two different approaches: i) applying BSS analysis to the abdECG (common approach), and ii) applying BSS analysis in the eECG (proposed approach). We employed the EFICA algorithm [40, 41] for BSS analysis in both cases. Cross-correlation is applied in all various combinations between the leads of the initial fECG (8) and the resulting sources after the application of the BSS (8); the maximum value is presented in ▶ Table 1. The average accuracy obtained for all simulated signals is 41.49% using the abdECG signals and 75.25% using the eECG signals (33.76% difference).

The EFICA technique for BSS analysis was selected on the basis of preliminary tests performed using the eECG extracted from the abdECG of a single simulated signal generated using 0 dB SNR. This signal was generated for this task only and it was not used elsewhere either in parameter identification or evaluation. For this signal, the normalized cross-correlation between the initial fECG and the extracted fECG was calculated (again as the maximum value of cross-correlation of all different combinations between the leads

of the initial fECG and the resulted sources after the application of the BSS technique), using 16 different BSS analysis techniques [41]. Also, the mean T/QRS ratio of the initial fECG and the extracted fECG was calculated. Ten different realizations of noise were implemented. The mean values obtained from this analysis are presented in ► Table 2. Based on these, the EFICA technique was selected, since it provided the best results for the combinatory index among all BSS analysis techniques (forth column), which was calculated as the average between the fECG correlation and the normalized smallest distance from the initial T/QRS ratio (i.e. the T/QRS ratio of the initial fECG).

The first series of abdECG signals was used to define the values of the parameters  $a$ ,  $b$  and  $c$ , for both maternal QRS elimination and fetal QRS detection steps of the first stage. In the first case (maternal QRS elimination step) we performed parameter analysis, varying  $a_1$ ,  $b_1$  and  $c_1$  in the range:  $a_1 \in \{0.5, 0.6, \dots, 1.5\}$ ,  $b_1 \in \{0.5, 0.6, \dots, 1.5\}$  and  $c_1 \in \{0.5, 0.6, \dots, 1.5\}$  and the best results (in terms of fHR extraction after the first stage of the methodology) for the first abdECG series were obtained using  $(a_1, b_1, c_1) (1.0, 1.0, 0.8)$ . Then, the parameters

used in the maternal QRS elimination step were set to the above values and the same procedure was followed in order to define the values of the parameters for the fetal QRS detection step, thus leading to  $(a_2, b_2, c_2) = (1.0, 1.4, 1.5)$ . These two sets of parameter values were used in the maternal QRS elimination and fetal QRS detection steps, respectively [29].

## 5. Results

Validation is performed for each of the stages of the proposed methodology (fHR extraction, fECG extraction, fECG analysis) and the results are presented separately. In all cases, validation was performed by comparing the obtained results with the known input, i.e. in the case of fECG extraction, the extracted fECG was correlated with the true fECG, which is known since it is generated from the simulator.

### 5.1 fHR Extraction

Three measures are used for the evaluation of fHR extraction: sensitivity  $Se = TP/(TP + FN)$

positive diagnostic value  $PDV = TP/(TP + FP)$  and accuracy  $Acc = TP/(TP + FP + FN)$ , where  $TP$  is the number of the true detected fetal R peaks,  $FP$  is the number of false detected fetal R peaks and  $FN$  is the number of missed fetal R peaks. The proposed methodology was evaluated using the signals of the 2–4 abdECG series. However, the results obtained from the three additional realizations of the abdECG signal are identical with the original signal (they are from the same signal with differences only in the ST waveform, which does not affect the fHR extraction procedure). Thus, only results for abdECG series 2 are presented.

The obtained results are 97.31%, 96.84% and 94.79% for average  $Se$ ,  $PDV$  and  $Acc$ , respectively (for the six signals of the second abdECG series). ► Table 3 presents the obtained results ( $TP$ ,  $FP$ ,  $FN$ ,  $Se$ ,  $PDV$  and  $Acc$ ) for each of the simulated signals, along with average results.

### 5.2 fECG Detection

The obtained fECG was compared with the true fECG: normalized cross-correlation is applied between the obtained fECG and the

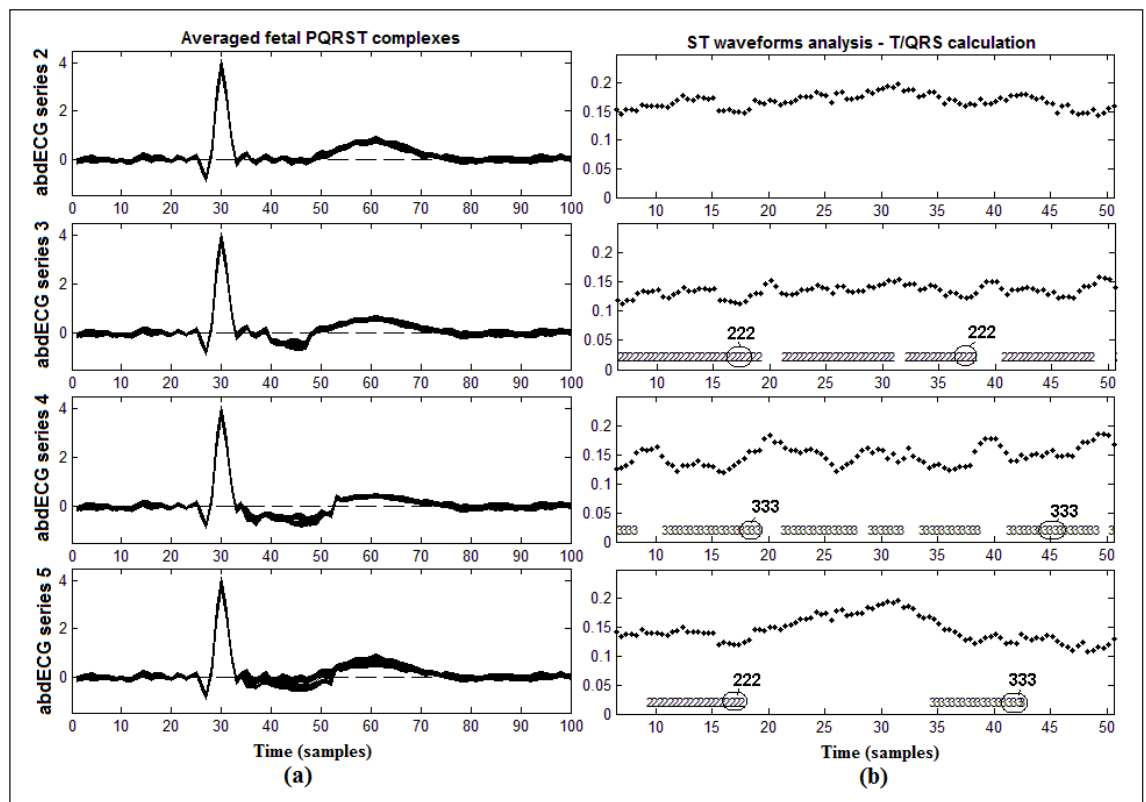


**Fig. 11** Application of the ST waveform analysis in the extracted fECG signal (2 dB SNR) for abdECG series 2–5. a) The averaged fPQRST complexes (each next average plotted upper the previous one), and b) the corresponding ST waveform analysis and T/QRS ratio calculation. Numbers 2 and 3 indicate annotation for biphasic ST waveforms of grade 2 and 3, respectively.

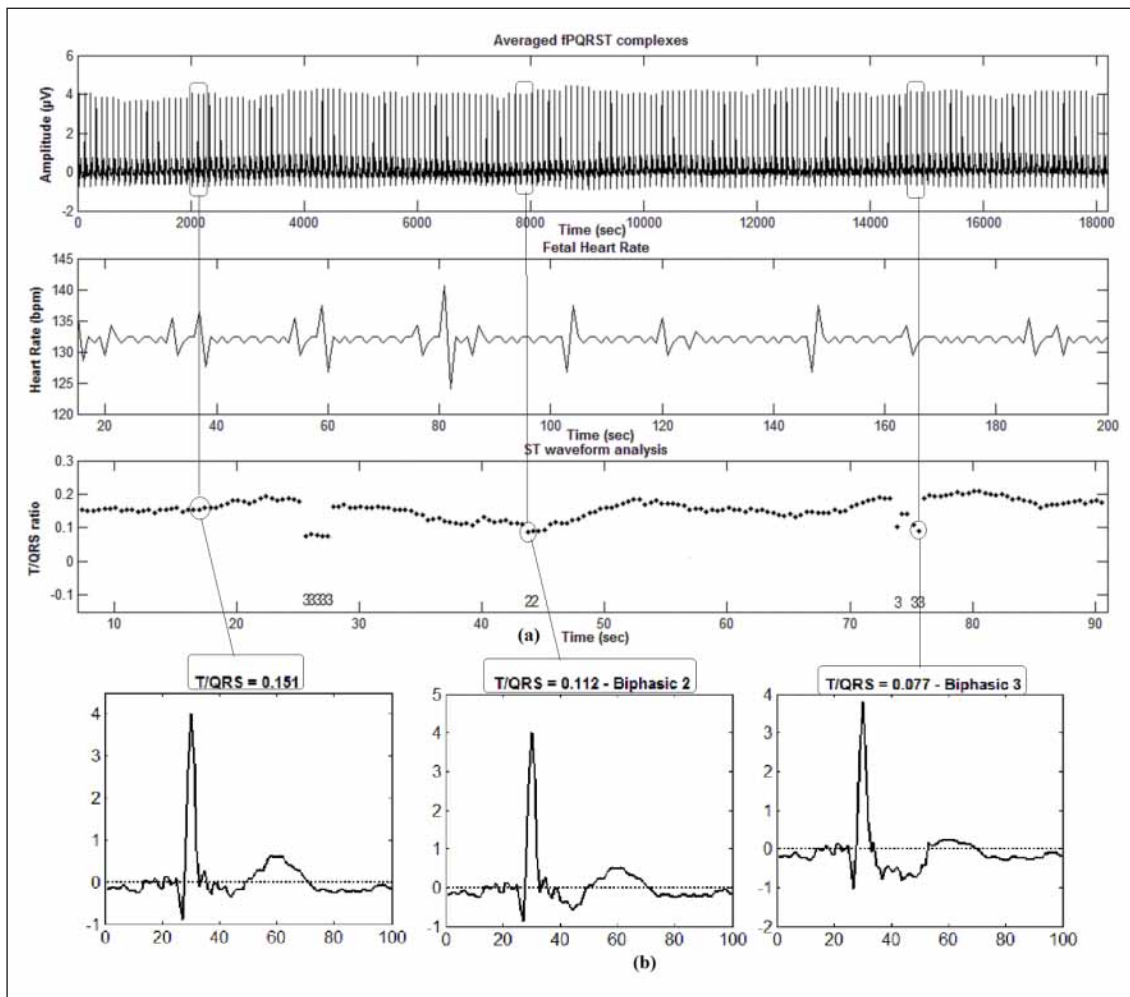


**Fig. 12** Snapshot of the application of the methodology. a) (from up to lower) The fPQRST complexes continuously plotted, the respective FHR and the T/QRS ratio and the annotation for each ST waveform, and b) the 3 fPQRST complexes corresponding to the specific time areas (dotted boxes)

eight fECG generated from the simulator (one for each recording channel). ▶ Table 4 presents the correlation between the extracted fECG in all different SNRs, with the eight channels of the fECG, generated from the simulator. The obtained results indicate that in all cases the extracted fECG presents high correlation with several of the simulated fECG channels. Also, the correlation value increases monotonically with the SNR used to generate the simulated signal, in all abdECG series.

### 5.3 T/QRS Ratio Calculation

▶ Table 5 presents a comparison between the T/QRS ratio calculated from the extracted fECG (final T/QRS ratio) and the T/QRS ratio calculated from the initial simulated fECG (initial T/QRS ratio). The initial T/QRS ratio is computed as follows:

- T/QRS is computed in each simulated fECG channel.
- A mean T/QRS is computed for every simulated fECG channel.
- The initial T/QRS is computed as the average value of all mean T/QRS ratio values (one for each simulated channel).

The final T/QRS is the mean value of the values of T/QRS computed for the extracted fECG. Ten different realizations of noise were implemented for each simulated abdECG (SNR value) and the mean value is computed.

### 5.4 ST Waveform Analysis

Our methodology classifies the ST waveforms in three different classes: normal, biphasic of grade 2 and biphasic of grade 3. The abdECG series 5 was used to evaluate this step: in each abdECG signal from this series 200 biphasic

ST waveforms of grade 2 and 200 biphasic ST waveforms of grade 3 were created. The sensitivity of the normal, biphasic of grade 2 and biphasic of grade 3 ST waveforms, for each simulated signal, is presented in ▶ Table 6.

▶ Figure 11 presents the application of the methodology in a simulated abdECG signal (2 dB SNR) of 1 minute duration, for all cases related to the ST waveform (i.e. normal, normal and biphasic of grade 2, normal and biphasic of grade 3, normal and biphasic of grades 2 and 3). In each case, the left plot presents the average fPQRST complex (each next fPQRST average plotted upper the previous one) and the right figure the T/QRS of each fECG beat along with the annotation of the respective ST waveform. Annotation is made automatically by the application, mentioned with numbers 2 and 3 for biphasic ST waveforms of grade 2 and 3, respectively, while no annotation is used for normal ST waveforms.

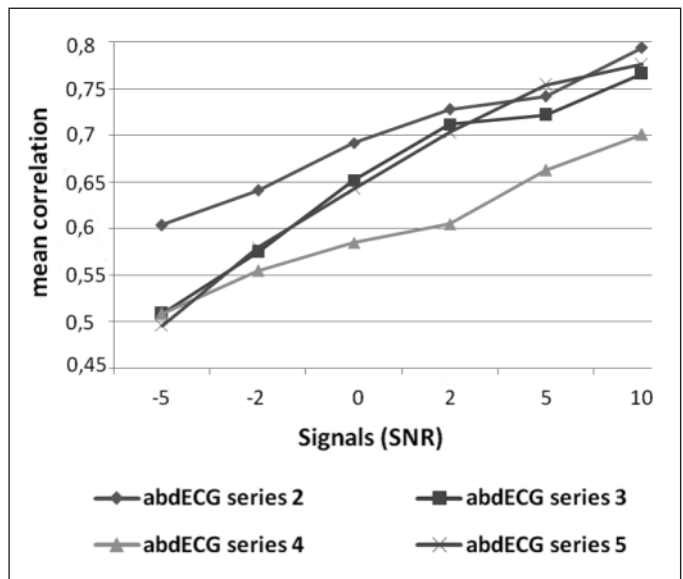
In ► Figure 12 a snapshot of the application of the methodology is presented. ► Figure 12a presents the fPQRST complexes (one next to other continuously), the respective fHR and the T/QRS ratio with the annotation of each ST waveform. In ► Figure 12b, we plot three specific fPQRST complexes with the corresponding ST analysis for the three different time intervals (noted in dotted boxes).

## 6. Discussion

A novel, non-invasive methodology for fetal health monitoring is presented. The proposed procedure acquires eight ECG signals from specific positions on the abdomen of the mother (multichannel abdECG). Then, extraction of fHR and fECG is carried out using a BSS approach, while further fECG ST waveform analysis is automatically performed to calculate the T/QRS ratio and classify the ST waveforms. Combining these signals and features with additional clinical information may contribute to fetal cardiac health assessment [1, 7]. Furthermore, the procedure is totally non-invasive, making thus fetal monitoring much easier for both doctors and pregnant women.

Several BSS techniques have been previously proposed for the fECG extraction from multichannel signals of the pregnant woman [14, 25, 26]. All these BSS approaches have been applied in the multichannel signals of abdomen and/or thorax without providing any pre-processing step. In our methodology, we followed a novel approach by applying BSS analysis in the eECG signal instead of the abdECG signal which is commonly used in the literature, since the strongest component of abdECG signals (mECG) is eliminated in the eECG and thus fECG is extracted with higher accuracy from it. This constitutes a major advantage of our approach as proven by our results (► Table 1). BSS techniques also suffer from the problem of permutation [24–26], i.e. after the application of BSS the signals of interest must be manually identified in the obtained sources. In our methodology we propose a novel approach to overcome this problem; fHR is initially extracted and employed later in the methodology for the identification of the sources obtained from the BSS analysis that include strong fECG interference. In this way, we combine the two approaches reported in the literature

**Fig. 13** Mean correlation values versus SNR curves, for the fECG extraction step



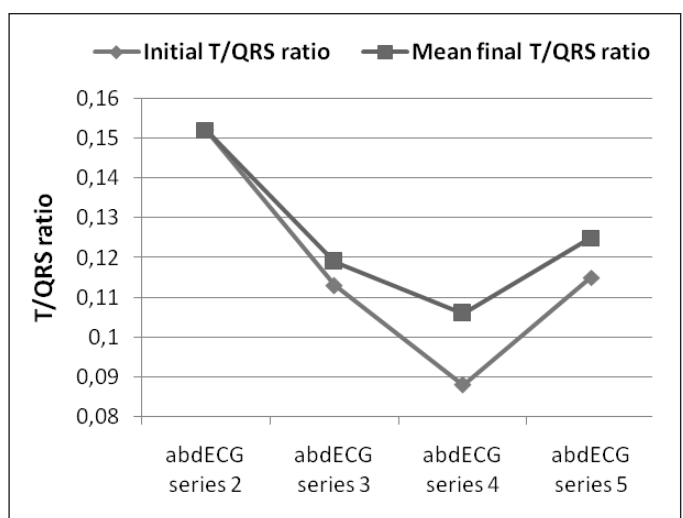
(direct extraction of fHR and extraction of fECG). This is a major advantage of our methodology compared to other approaches based on BSS analysis, since it addresses the permutation problem and allows a fully automated analysis. In addition, the EFICA technique has not been previously employed for fECG extraction and has shown to be more efficient than other approaches.

A method similar to ours for extracting the fECG from abdominal composite signals has been proposed by Sato et al. [43]; the method consists of the cancellation of the mECG and subsequent application of BSS with a reference signal in the eECG. The

method is able to extract the P and T waves in addition to the R wave. Major limitations of the method are: the need for parallel recording of the ultrasonic Doppler signal that is used as the reference signal, the lack of denoising stage in cases of very noisy signals, the use of a large number of electrodes (14) that makes the application difficult and non-ergonomic and the inability of the method to perform automated ST waveform analysis.

The proposed methodology allows automated ST waveform analysis that is based on totally non-invasive signals (abdECG recordings) instead of the invasive ones used in clinical practice (fetal scalp electrode). Non-

**Fig. 14** T/QRS ratio and the difference between the initial T/QRS ratio and final (mean) T/QRS ratio in all cases (series 2 to 5)



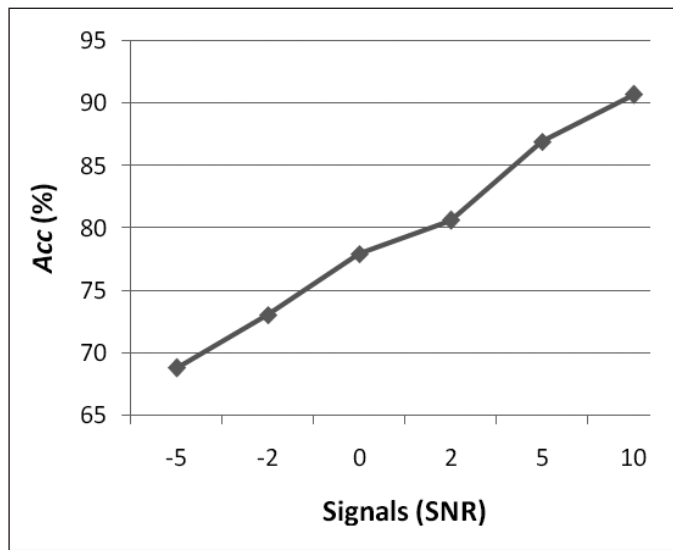


**Fig. 15**  
Classification Acc vs SNR curves, for the calculation of T/QRS ratio

invasive automated ST waveform analysis has not been previously presented in the literature; Sato et al. only presented morphological and timing correlation ECG analysis [43].

The results obtained from the fHR extraction step (►Table 3) clearly demonstrate the effectiveness of the method. High accuracy is shown for all SNR cases except for these with unexpectedly big amount of noise, with SNR of  $-5$  dB or lower, in which the fECG is hardly visible. As clearly demonstrated in ►Table 3, accuracy increases monotonically with the SNR.

The fECG detection results (►Fig. 13) also indicate high efficiency in fECG extraction. Again, the results appear to improve monotonically with respect to the SNR; this is shown in ►Figure 13. The presence of biphasic grade 2 and 3 ST waveforms slightly reduces the efficiency of the methodology in most cases; lower mean normalized cross-correlation presents is obtained.

Satisfactory results are also presented regarding the correctness in the T/QRS ratio calculation (►Fig. 14). The initial T/QRS ratio and the final (mean) T/QRS ratio differ slightly in all cases and this difference is not considered crucial for fetal cardiac health assessment [1], while for the abdECGs with normal ST waveforms (abdECG series 2) the difference is zero. However, this difference increases in case of biphasic grade 2 ST waveforms (adbECG series 3) and further increases in case of biphasic grade 3 ST waveforms (adbECG series 4), while in case of mixture of normal and biphasic grade 2 and 3

ST waveforms (abdECG series 5), the difference lies between the previous two cases. This finding, presented graphically in ►Figure 14, clearly demonstrates that the closer-to-normal the analyzed ST waveform is, the more efficient the calculation of T/QRS ratio. This implies that the proposed methodology is sensitive to the complexity of the abdECG signal, i.e. as complexity increases, efficiency is reduced.

In addition, the accuracy in T/QRS calculation has been estimated as the percentage (%) deviation between the initial T/QRS ratio and the final (mean) T/QRS ratio, as:

$$Acc = 100 \left( 1 - \frac{|initial - final|}{initial} \right) \% .$$

According to this metric, the accuracy of the T/QRS ratio calculation procedure is 100%, 94.96%, 83.02% and 92%, for the abdECG series 2, 3, 4 and 5, respectively, while the average accuracy for all abdECG signals used for evaluation (all abdECG series) is 92.49%. Classification of the ST waveforms has been performed on the abdECG series 5, since this includes ST waveforms from all three classes (normal, biphasic grade 2 and biphasic grade 3). Again the accuracy in classification was proven to be high and to increase monotonically with the increase in the SNR used to generate the simulated signals (►Fig. 15).

The extraction of fECG and/or fHR extraction from the abdECG presents many technical difficulties that have been addressed in part by the proposed methodology. The abdominal leads record a composite signal

(abdECG), consisting of the contributions from both the mECG and the fECG as well as sources of interference including intrinsic noise from the recorder, noise from electrode-skin contact and movement, baseline drift (DC shift), A/C interference noise, uterine contractions activity, etc. Furthermore, fECG occasionally overlaps with mECG, while the fECG signal may vary based on the gestational age, the position of the fetus [42] and the positioning of the electrodes [44].

There are only few approaches presented in the literature using an embedded noise treatment strategy [13, 23, 46], while most of published techniques do not cope with noisy recordings and thus cannot be used in real clinical practice. Our methodology is designed to integrate various denoising techniques in several of its stages.

No standard electrode positioning for optimal fECG acquisition has been previously reported [44]. The methodology proposed here employs eight leads in specific locations on the mother's abdomen and has shown good results when evaluated using simulated signals based on the fetus' usual position. However, the quality of signals may vary mainly because of different fetal positions, fetal movements especially in the early stages of pregnancy, uterine contractions and changes in mECG. Further research is therefore needed in order to evaluate the performance of the methodology in clinical practice.

The lack of a uterine contraction recording is a limitation of the proposed procedure. Uterine contraction might affect fHR; the incorporation of an external transducer for the recording of the uterine activity is considered essential for the detection of all types of periodic fHR changes and would lead to a more accurate and efficient monitoring technique [30, 31].

The equipment used in the proposed methodology to record fECG is of low cost and may be used in conjunction with wearable devices; this is an important advantage of the proposed methodology. The non-invasive nature of the approach combined with its wearability makes it appropriate for healthcare support of pregnant women at remote settings. Telemonitoring of fECG in combination with automated analysis may prove to be important in antenatal surveillance of high-risk pregnancies. Additional features important for fetal monitoring may easily be

extracted from the results obtained from our methodology (fHR, fECG, T/QRS ratio, ST waveform classification). Based on parameters related to fHR, such as baseline fHR, fHR variability, reactivity and presence of accelerations and decelerations, fHR can be classified as reassuring, non-reassuring and abnormal. ST events can also be characterized as normal, episodic, baseline or biphasic. However, the above parameters have not been included in the current work since the evaluation is performed using only simulated signals that present specific characteristics (such as fHR) and do not include abnormalities. This is a limitation of this study and evaluation using real abdECG recordings is very important to fully exploit the potential of the proposed methodology. In addition, the proposed methodology is able to extract mECG and mHR and thus may be useful in monitoring of the mother using sophisticated techniques in arrhythmia [47] and/or ischemia detection [48]. The employment of additional features such as those described above, the application and evaluation of the methodology to real abdECG recordings as well as its use in maternal monitoring will be addressed in future communications.

## 7. Conclusions

A methodology for the monitoring of the fetal cardiac condition during pregnancy based on abdominal ECG recordings has been presented. Each step of the procedure was evaluated using simulated signals and the results indicate high accuracy. The automated extraction of the fECG from the abdECG and the incorporation of features extracted from it (such as T/QRS ratio and ST waveform analysis) can reveal additional information for the fetal cardiac health. A limitation of our study is that only simulated signals have been employed, and further evaluation with real recordings is required.

## Acknowledgments

We are grateful to Dr. Kostas Zikopoulos, Associate Professor in Obstetrics and Gynecology, University of Ioannina, Ioannina, Greece for his help with the introduction of the manuscript.

## References

1. Sundström AK, Rosén D, Rosén KG. Fetal surveillance. Chicago: Textbook, Neovanta Medical AB; 2006. [http://www.fda.gov/ohrms/dockets/AC/05/briefing/2005-4150b1\\_06\\_NEOVENTA%20STAN%20S31%20TRAINING%20TEXT%20BOOK.PDF](http://www.fda.gov/ohrms/dockets/AC/05/briefing/2005-4150b1_06_NEOVENTA%20STAN%20S31%20TRAINING%20TEXT%20BOOK.PDF)
2. Smith JF. Fetal health assessment using prenatal diagnostic techniques. *Curr Opin Obstet Gynecol* 2008; 20: 152–156.
3. Tempfer C, Hefler L, Husslein P. Modern intrapartum fetal monitoring: room for improvement? *Arch Gynecol Obstet* 2007; 276: 99–100.
4. Alfirevic Z, Devane D, Gyte GM. Continuous cardiotocography (CTG) as a form of electronic fetal monitoring (EFM) for fetal assessment during labour. *Cochrane Database Syst Rev* 2006; 3: CD006066
5. Amer-Wählin I, Yli B, Arulkumaran S. Foetal ECG and STAN technology – A review. *European Clinics in Obstetrics and Gynaecology* 2005; 1: 61–73.
6. Rosn KG, Amer-Wählin I, Luzietti R, Norn H. Fetal ECG waveform analysis. *Best Practice and Research Clinical Obstetrics and Gynaecology* 2004; 18: 485–514.
7. Su LL, Chong YS, Biswas A. Use of Fetal Electrocardiogram for Intrapartum Monitoring. *Annals Academy of Medicine* 2007; 36: 416–420.
8. Westgate J, Harris M, Curnow JS, Greene KR. Plymouth randomized trial of cardiotocography only versus ST waveform plus cardiotocogram for intrapartum monitoring in 2400 cases. *Am J Obstet Gynecol* 1993; 169: 1151–1160.
9. Neilson JP. Fetal electrocardiogram (ECG) for fetal monitoring during labour. *Cochrane Database of Systematic Reviews* 2006, Issue 2. (Art. No.: CD000116. DOI: 10.1002/14651858.CD000116.pub2)
10. Ferrario M, Signorini MG, Magenes G. Comparison between fetal heart rate standard parameters and complexity indexes for the identification of severe intrauterine growth restriction. *Methods Inf Med* 2007; 46 (2): 186–190.
11. Turan S, Turan OM, Berg C, Moyano D, Bhide A, Bower S, Thilaganathan B, Gembruch U, Nicolaidis K, Harman C, Baschat AA. Computerized fetal heart rate analysis, Doppler ultrasound and biophysical profile score in the prediction of acid-base status of growth-restricted fetuses. *Ultrasound Obstet Gynecol* 2007; 30: 750–756.
12. Newnham JP, Doherty DA, Kendall GE, Zubrick SR, Landau LL, Stanley FJ. Effects of repeated prenatal ultrasound examinations on childhood outcome up to 8 years of age: follow-up of a randomised controlled trial. *Lancet* 2004; 364 (9450): 2038–2044.
13. Pieri JE, Crowe JA, Hayes-Gill BR, Spencer CJ, Bhogal K, James DK. Compact long-term recorder for the transabdominal foetal and maternal electrocardiogram. *Med Biol Eng Comput* 2001; 39: 118–125.
14. Zarzoso V, Nandi AK. Noninvasive Fetal Electrocardiogram Extraction: Blind Separation versus Adaptive Noise Cancellation. *IEEE Trans Biomed Eng* 2001; 48: 12–18.
15. Richter M, Schreiber T, Kaplan DT. Fetal ECG extraction with nonlinear state space projections. *IEEE Trans Biomed Eng* 1998; 45: 133–137.
16. Camps-Valls G, Martinez-Sober M, Soria-Olivas E, Guerrero-Martinez J, Calpe-Maravilla J. Foetal ECG recovery using dynamic neural networks. *Artificial Intelligence in Medicine* 2004; 31: 197–209.
17. Barros AK, Cichocki A. Extraction of Specific Signals with Temporal Structure. *Neural Computation* 2001; 13: 1995–2003.
18. Azad KAK. Fetal QRS Complex Detection from Abdominal ECG: A Fuzzy Approach. In: *Nordic Signal Processing Symposium (NORSIG). Proceedings of the Annual International Conference of the IEEE*; 2000, Sweden. September 22–24; 2000. pp 275–278.
19. Assaleh K, Al-Nashash H. A Novel Technique for the Extraction of Fetal ECG Using Polynomial Networks. *IEEE Trans Biomed Eng* 2005; 52: 1148–1152.
20. Karvounis EC, Tsipouras MG, Fotiadis DI, Naka KK. An Automated Methodology for Fetal Heart Rate Extraction from the Abdominal Electrocardiogram. *IEEE Trans. on Information Technology in Biomedicine* 2007; 11: 628–638.
21. Khamene A, Negahdaripour S. A New Method for the Extraction of Fetal ECG from the Composite Abdominal Signal. *IEEE Trans Biomed Eng* 2000; 47: 507–516.
22. Karvounis EC, Papaloukas C, Fotiadis DI, Michalis LK. Fetal Heart Rate Extraction from Composite Maternal ECG Using Complex Continuous Wavelet Transform. In: *Computers in Cardiology, ICA 2004. Proceedings of the 5th Annual International Conference of the IEEE*; 2004, Chicago (USA), September 22–24; 2004. pp 19–22.
23. Ibrahimy MI, Ahmed F, Mohd Ali MA, Zahedi E. Real-Time Signal Processing for Fetal Heart Rate Monitoring. *IEEE Trans Biomed Eng* 2003; 50: 258–262.
24. Cichocki A, Amari S. *Adaptive Blind Signal and Image Processing*. England: John Wiley & Sons; 2002.
25. Zarzoso V, Nandi AK, Bacharakis E. Maternal and Foetal ECG Separation using Blind Source Separation Methods. *IMA J Math Appl Med and Biol* 1997; 14: 207–225.
26. Lathauwer LD, Moor BD, Vandewalle J. Fetal Electrocardiogram Extraction by Blind Source Subspace Separation. *IEEE Trans Biomed Eng* 2000; 47: 567–572.
27. Jafari MG, Chambers JA. Fetal Electrocardiogram Extraction by Sequential Source Separation in the Wavelet Domain. *IEEE Trans Biomed Eng* 2005; 52: 390–400.
28. Lu W, Rajapakse JC. ICA with reference. *Neurocomput* 2006; 69: 2244–2257.
29. Karvounis EC, Tsipouras M, Fotiadis DI. Detection of Fetal Heart Rate through 3D Phase-Space Analysis from Multivariate Abdominal Recordings. *IEEE Trans Biomed Eng* 2009; 56 (5): 1394–406.
30. Jezewski J, Matonia A, Kupka T, Wrobel J. Fetal monitoring with online processing of electrocardiographic signals. In: *EMBECC, Prague, November 20–25; 2005*. pp 523–526.
31. Taylor MJO, Smith MJ, Thomas M, Green AR, Cheng F, Oseku-Afful S, Wee LY, Fisk NM, Gardiner HM. Non-invasive fetal electrocardiography in singleton and multiple pregnancies. *British J Obstet Gynecol* 2003; 110: 668–678.
32. Qinetiq non-invasive fetal ECG technology. London. Available from: <http://www.qinetiq.com/>

- home/newsroom/news\_releases\_homepage/2003/3rd\_quarter/scientists.html
33. Monica AN24 Fetal Holter (Monica Healthcare Ltd). Nottingham, UK. Available from: <http://www.monicahealthcare.com>
  34. Sameni R, Clifford GD, Jutten C, Shamsollahi MB. Multichannel ECG and Noise Modeling: Application to Maternal and Fetal ECG Signals. EURASIP Journal on Advances in Signal Processing, vol. 2007. (Research Article ID 43407, pp 1–14, , doi: 10.1155/2007/43407).
  35. Zhang Q. Matlab Package for Robust and Efficient Location of T-Wave Ends in ECG and Its Evaluation with PhysioNet Data 2005. Available from: <http://www.irisa.fr/sosso/zhang/biomedical/>
  36. Goring DG, Nikora VI. Despiking Acoustic Doppler Velocimeter Data. J Hydr Engrg 2002; 128: 117–126.
  37. Mori N, Suzuki T, Kakuno S. Noise of acoustic Doppler velocimeter data in bubbly flow. Journal of Eng Mech 2007; 133: 122–125.
  38. Abboud S, Sadeh D. Spectral analysis of the fetal electrocardiogram. Comput Biol Med 1989; 19: 409–415.
  39. Aminghafari M, Cheze N, Poggi JM. Multivariate de-noising using wavelets and principal component analysis. Computational Statistics & Data Analysis 2006; 50: 2381–2398.
  40. Koldovský Z, Tichavský P, Oja E. Efficient Variant of Algorithm FastICA for Independent Component Analysis Attaining the Cramér-Rao Lower Bound. IEEE Trans. on Neural Networks 2006; 17: 1265–1277.
  41. Cichocki A, Amari S, Siwek K, Tanaka T, Anh Huy Phan AH, Zdunek R. ICALAB – MATLAB Toolbox Ver. 3 for signal processing. Available from: [http://www.bsp.brain.riken.jp/ICALAB/ICALAB\\_SignalProc/](http://www.bsp.brain.riken.jp/ICALAB/ICALAB_SignalProc/)
  42. Golbach EGM, Stinstra JG, Grot P, Peters MJ. Reference values for fetal MCG/ECG recordings in uncomplicated pregnancies. In: Biomagnetism, 2000. Proceedings of the 12th Annual International Conference; 2000, Espoo, Finland; 2000. pp 595–598.
  43. Sato M, Kimura Y, Chida S, Ito T, Katayama N, Okamura K, Nakao M. A Novel Extraction Method of Fetal Electrocardiogram from the Composite Abdominal Signal. IEEE Trans Biomed Eng 2007; 54: 49–58.
  44. Vrins V, Jutten C, Verleysen M. Sensor Array and Electrode Selection for Non-invasive Fetal Electrocardiogram Extraction by Independent Component Analysis. In: Computers in Cardiology, ICA 2004. Proceedings of the 5th Annual International Conference of the IEEE; 2004, Chicago (USA), September 22–24; 2004. pp 1017–1024.
  45. Martens SMM, Rabotti C, Mischi M, Sluijter RJ. A robust fetal ECG detection method for abdominal recordings. Physiol Meas 2007; 28: 373–388.
  46. Al-Zaden A, Al-Smadi A. Extraction of foetal ECG by combination of singular value decomposition and neuro-fuzzy inference system. Phys Med Biol 2006; 51: 137–143.
  47. Tsipouras MG, Voglis C, Fotiadis DI. A Framework for Fuzzy Expert System Creation-Application to Cardiovascular Diseases. IEEE Trans Biomed Eng 2007; 54: 2089–2105.
  48. Papaloukas C, Fotiadis DI, Likas A, Michalis LK. Automated methods for ischemia detection in long-duration ECGs. Cardiovascular Reviews and Reports 2003; 24: 313–320.